

Supporting Information

**Biomarkers-triggered, spatiotemporal controlled DNA nanodevice
simultaneous assembly and disassembly**

Tingting Zhao¹, Yi Fang¹, Xuyang Wang², Lei Wang¹, Yujuan Chu¹, Wenxiao Wang*¹

¹Shandong Province Key Laboratory of Detection Technology for Tumor Makers, College of Chemistry and Chemical Engineering, Linyi University, Linyi 276000, P.R. China.

²Biomedical Science College, Shandong First Medical University & Shandong Academy of Medical Sciences, Jinan 250000, P. R. China.

Table of contents

Experimental Section	3
Table S1. DNA sequences.....	10
Figure S1. TEM of AuNPs.....	11
Figure S2. Zeta potential of AuNPs and TNPa.....	12
Figure S3. the stability of the TNPa.....	13
Figure S4. UV absorption spectrum of AuNPs and TNPa.....	14
Figure S5. Size of TNPa.....	15
Figure S6. DLS characterizes TNPa responsive nucleolin assembly.....	16
Figure S7. DLS characterization of TNPa assemblies in response to APE1 disassembly.....	17
Figure S8. Colorimetric verification of TNPa assembly and disassembly processes.....	18
Figure S9. The universality of DNA nanodevices.....	19
Figure S10. Selectivity of TNPa for nucleolin.....	20
Figure S11. Selectivity of TNPa assembly for APE1.....	21
Table 2. Detection results of nucleolin spiked in human serum samples.....	22
Table 3. Detection results of APE1 spiked in human serum samples.....	23
Figure S12. MTT assay.....	24
Figure S13. Hemolysis analysis of TNPa.....	25
Figure S14. Reagent kit analysis of nucleolin and APE1 concentrations.....	26
Figure S15. Fluorescence images of tumor-bearing mice tail vein injected with TNPa.....	27

EXPERIMENTAL SECTION

Materials and Reagents. All oligonucleotides were obtained from Shanghai Sangon Biological Engineering Technology and Services Co., Ltd. (Shanghai, China). All the synthetic oligonucleotides were HPLC purified and freeze-dried by the supplier. Their sequences were listed in Supporting Information (Table S-1). All oligonucleotides were received as powders and centrifuged so that they would reside at the bottom of the containers. The powder was then dissolved with 10 mM phosphate-buffered saline (PBS, pH 7.4) to give stock solutions of 100 μ M. Sodium chloride (NaCl), potassium chloride (KCl), magnesium chloridehexahydrate ($MgCl_2$), calcium chloride ($CaCl_2$), Tris-HCl, disodium hydrogen phosphate (Na_2HPO_4), dibasic sodium phosphate (Na_2HPO_4), Chloroauric acid ($HAuCl_4$), Sodium citrate ($C_6H_5Na_3O_7$) were purchased from Sigma-Aldrich. Apurinic-Apyrimidinic Endonuclease 1 (APE1) and nucleolin were purchased from New England Biolabs. APE1 inhibitor APE1-IN-1, doxorubicin hydrochloride (DOX) and 3-(4,5-dimethylthiazol-2-yl)-2,5-diphenyltetrazolium bromide (MTT) were purchased from Sigma-Aldrich. Dulbecco's modified Eagle's medium (DMEM), fetal bovine serum (FBS), penicillin-streptomycin and trypsin were obtained from GIBCO Invitrogen Corp. Ultrapure water was obtained from Milli-Q apparatus (Millipore, Bedford, MA). All reagents are analytical grade and solutions were prepared using ultrapure water (specific resistance of 18 M Ω cm, Milli-Q Gradient System, Millipore, Bedford, MA).

Apparatus. The morphology and size of nanoparticles were measured with transmission electron microscopy (TEM) (JEM-2100, Hitachi, Japan). UV-vis absorption spectroscopy was measured by Cary60 UV-vis spectrophotometer. Zeta

potential and hydrodynamic diameters were analyzed by Zetasizer Nano ZS90 (Malvern, UK). Fluorescence spectrum was examined by fluorescence spectrophotometer (FL970). The native polyacrylamide gels were imaged with ChemiDoc MP Imaging Systems (Tanon 1600). Intracellular imaging was determined through confocal laser scanning microscope (LeicaTCS + LeicaAM). *In vivo* imaging was determined through IVIS.

Synthesis of 13 nm AuNPs. 13 nm AuNPs were synthesized following a previously reported protocol. Briefly, 98 ml of Millipore water and 2 ml of a 50 mM HAuCl₄ solution were mixed in a clean 200 ml two-neck round-bottom flask equipped with a reflux condenser and stopper. The flask was heated to reflux, whereupon 10 ml of 38.8 mM sodium citrate was quickly added to the reaction mixture. The color of the solution was observed to change to deep red in 1 min. The system was refluxed further for 20 min, and then allowed to cool to room temperature while stirring. In a typical reaction, the concentration of the final AuNP solution is ~10 nM.

Functionalization of AuNPs with DNA. First, thiolated DNA samples (b*c*de) were used as received without further treatment (i.e. no DTT or TCEP treatment). Second, DNA1, DNA2 and DNA3 were mixed to a final ratio of 1: 1.2: 1.2. The solution was incubated at 37°C for 2 h. The solution was stored at 4°C overnight to allow full hybridization. Third, the mixture (100 μM, 3 μL) was mixed AuNPs (10 nM, 100 μL). The DNA1/DNA2/DNA3 mixture was then placed in a laboratory freezer (set at -20 °C) for 2 h, followed by thawing at room temperature. Excess DNA1/DNA2/DNA3 was removed by centrifugation and washing with PBS. Finally,

TNP_a was dispersed in 200 μ L PBS for further use.

Transmission electron microscopy. AuNPs, TNP_a and TNP_a assembly were analyzed using a Hitachi HD-2300 scanning transmission electron microscope in either SE or TE modes with an accelerating voltage of 200 kV. Samples were dispersed onto copper mesh by drop-casting a dilute solution containing AuNPs, DNA nanodevice and DNA nanodevice assembly directly onto copper mesh.

Dynamic light Scattering (DLS) and zeta potential measurements. Zeta potential and dynamic light scattering measurements of hydrodynamic radii were made on a Malvern Zetasizer Nano-ZS (Malvern Instruments). Results were averaged over ten measurements.

UV-vis spectroscopy. Concentration of nucleic acid and AuNPs were determined via UV-vis spectroscopy in 100 μ L quartz cuvettes with a path length of $d = 1$ cm.

8 % Native PAGE. Non-denaturing polyacrylamide gel electrophoresis (PAGE) was used to further confirm DNA1/DNA2/DNA3 responds to nucleolin assembly and reassembly after responding to APE1. The reaction process was conducted as follow: DNA1/DNA2/DNA3 react with mRNA (1 nM) or mRNA and APE1 ($0.5 \text{ U} \cdot \text{mL}^{-1}$) at 37 °C for 12 h, respectively. After the reaction, the sample was loaded into a 8 % native PAGE, and the electrophoresis was carried in 1 \times Tris-borate-EDTA (TBE) buffer (89 mM tris(hydroxymethyl)aminomethane, 2 mM ethylenediaminetetraacetic acid and 89 mM boric acid, pH 8.0) at 100 V for 2.5 h. The gel was stained by SYBR Green II for 30 min and scanned by a ChemiDoc™ MP System (Bio-Rad).

Fluorescence assay. For vitro fluorescence assays, a mixture of TNP_a 10 μ L, 1 nM,

10 nM mRNA and 0.5 U APE1 in $1 \times$ NEB buffer4 (50 mM KAc, 20 mM Tris-Ac, 10 mM Mg (Ac)₂, 1 mM DTT). Fluorescence intensity of samples was measured separately at 494 nm excitation, 520 nm emission (FAM) and 646 nm excitation, 664 nm. Time-dependent fluorescence changes were recorded separately at a fixed wavelength of 520 nm and 664.

Cell cultivation. HeLa cells were cultured in Dulbecco's modified Eagle's medium (DMEM) and fetal bovine serum (FBS; 10%) supplemented with penicillin/streptomycin (1%) at 37 °C in 5% CO₂, 70% humidity, and reseeded every 2-4 days to maintain subconfluency. When HeLa cells reached about 90% confluency, they were split into 24-well plates at a volume ratio of 1:4 by using a standard trypsin-based technique with the final cell concentration of 8×10^4 cells mL⁻¹. HeLa cells were incubated in 24-well plates in culture media at a concentration that allowed 90% confluence in 48 h.

MTT cell viability assay. HeLa cells (5×10^3 cells/well) were seeded in 96-well plates and cultured for 24 h. The cells were exposed to the DNA nanodevicesal gold/DNA for 24 h, followed by adding with 50 μ L of the MTT solution (1 mg/mL) and incubating at 37 °C for additional 4 h. Afterward, the media were removed, and the cells were dissolved by 150 μ L of DMSO. The absorbance was determined at the wavelength of 570 nm using the microplate reader. The cell viability ($A/A_0 \times 100\%$) was calculated, where A and A₀ were the absorbance at 570 nm after treatment with and without the testing samples, respectively.

Cell Imaging. Cells were plated with a DMEM medium (1.0 mL) in glass-bottom

culture dishes for 24 h. After washing twice with PBS, cells were incubated with 3 nM TNPa for 10 min, 30min, 60min, 90 min, 120 min and were then washed three times with PBS. The fluorescence images of cells were collected using LeicaTCS + LeicaAM laser scanning confocal microscopy with a 63× objective. The FAM and Cy5 were measured under the excitation of 488 nm and 633 nm, respectively. For cell imaging assay, TNPa treated cells and control cells were all cultured in 1 mL culture medium. Then the procedure was as described above. For APE1 inhibitors assay, HeLa cells were incubated with different concentrations of inhibitors for 3 h.

Tumor allografts, injection of medication and *in vivo* fluorescence imaging. We have used a HeLa cultured in DMEM+10% Newborn calf serum (Gibco, Life Technologies). Female balb/c nude mice, weigh 17-19 g, were bred and housed with a standardized chow diet with free access to water ad libitum, housed on a 12/12-h light/dark cycle. Prior to injection, tumor cells were trypsin detached, washed twice, and resuspended in PBS to a final concentration of 5×10^5 viable cells/mL. The cell suspension was maintained on ice until injection. Mice were anesthetized with 5% Isoflurane laid on their backs, and injected with 100 μ L cell suspension. HeLa cells (100 μ L) was injected into the right thigh over 15 min using a microsyringe pump controller. Tumor growth was monitored weekly using digital callipers, and tumor volume was calculated according to the formula: $A \times B^2 \times 0.5 = \text{mm}^3$. Imaging studies were performed after six days after implant when tumors reached. When the tumor reaches 150 mm^3 , 3 nM TNPa are injected into the body for imaging. we next tested the ability of TNPa to detect and image endogenously expressed nucleolin and APE1

sequentially in mice. For *in vivo* fluorescence imaging experiments TNPa (3 nM) were solved in PBS for Fluorescence signal collection. Mice under anesthesia were injected with drugs (20 μ L, 10 nM) into the tumors and imaged 10 min after injection. Data collection began at 1, 2, 4, and 6 hours after intratumoral injection of 20 μ L with the Cy5 and FAM label in female balb/c nude mice. 1, 2, 4, and 6 hours post-injection, the *in vivo* imaging of tumor was measured by a *in vivo* imaging system (410-790 nm IVIS). Female balb/c nude mice were anesthetized with 3% isoflurane and oxygen and positioned on the imager console. We used two channels to detect fluorescence signals, namely Cy5 (649nm-666nm) and FAM (495nm-519nm). The images of tumors were acquired at 1 h intervals from injection up to 0 hours. After last images (8 hours intratumoral injection), tumors were extracted and fixed in 4% paraformaldehyde. Normalization and quantification of the images analysis were carried out using image J. 3D image reconstruction and image analysis were also carried out using image J.

Reagent kit analysis of nucleolin and APE1 concentrations. Taking nucleolin as an example, nucleolin antibody in a 96 well microplate to create a solid-phase carrier. Add standards or specimens to each microplate, where the skin nucleolin binds to the antibody attached to the solid-phase carrier. Then, add biotinylated skin nucleolin antibody. Wash the unbound biotinylated antibody, add HRP labeled avidin, thoroughly wash again, and add TMB substrate for color development. TMB is converted into blue under the catalysis of peroxidase, and finally into yellow under the action of acid. The depth of color is positively correlated with the skin nucleolin in the sample. Measure the absorbance (O.D. value) using an ELISA reader at a wavelength of

450nm and calculate the sample concentration.

Table S1. DNA sequences (from 5' to 3') used in this work.

b*c*de: HS-TTTT TTT TCC ACC ACC ACC ACG ACG A CGA CGA CGA CGA

CGA CGA TTT TTT TG TGT CTT TGG C(AP)AT ACT T

ab: GGT GGT GGT GGT TGT GGT GGT GGT GGT GCT GCT

c: TCG TCG TCG TCG TCG TCG

a*b*: TGA TCA AGT ATG CCA AAG ACA CAC TCG CTA CA

FAM-a*b*: GGT GGT GGT GGT TGT GGT GGT GGT GGT GCT GCT(FAM)

Cy5-b*c*de: HS-TTTT TTT TCC ACC ACC ACC ACG ACG A CGA CGA CGA

CGA CGA CGA TTT TTT TG TGT CTT TGG C(AP)AT ACT T(Cy5)

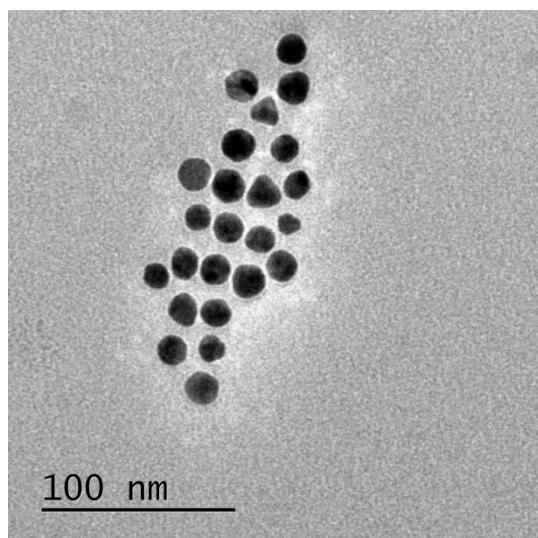


Figure S1. TEM of AuNPs.

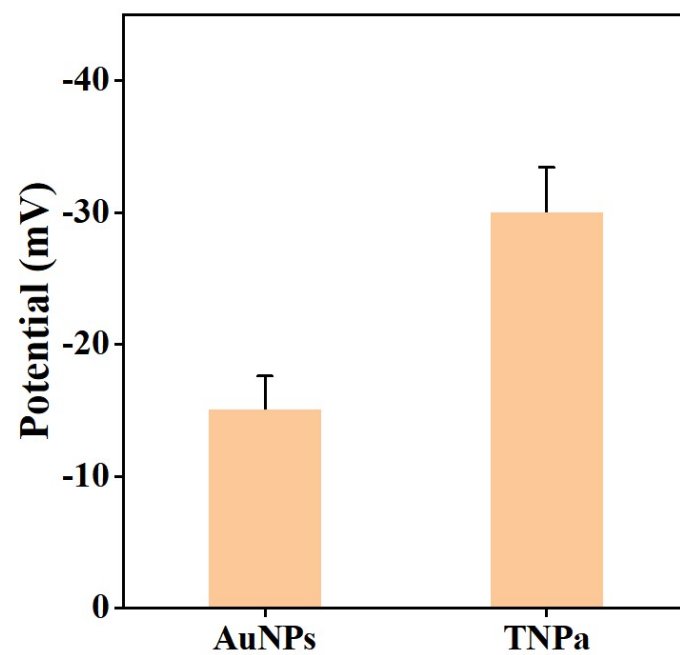


Figure S2. Zeta potential of AuNPs and TNPa.



Figure S3. Gel electrophoresis characterizes the stability of the TNPa. (a) 10 nM TNPa, (b) 10 nM TNPa + 10% serum, (c) 10 nM TNPa + 5 U mL⁻¹ DNase I. There are no obvious DNA degradation products below bands b and c, indicating that TNPa has high stability.

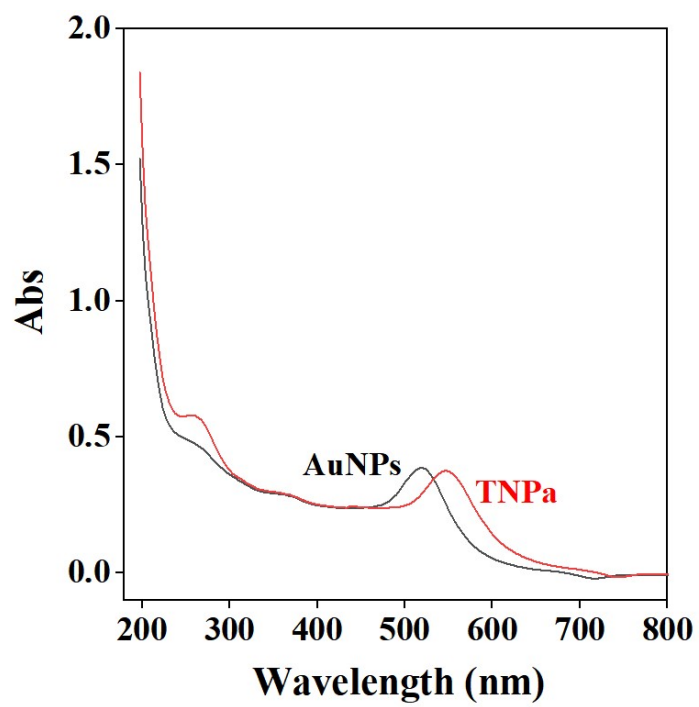


Figure S4. UV absorption spectrum of AuNPs (black) and TNPa (red).

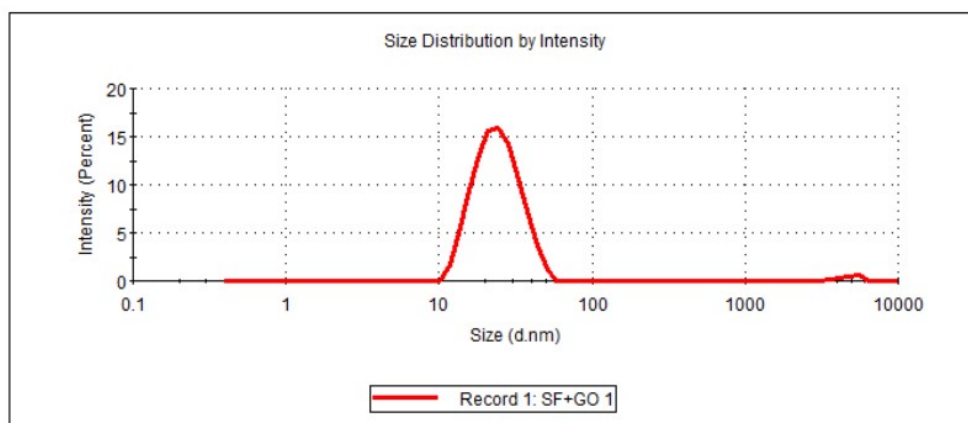


Figure S5. Size of TNPa.

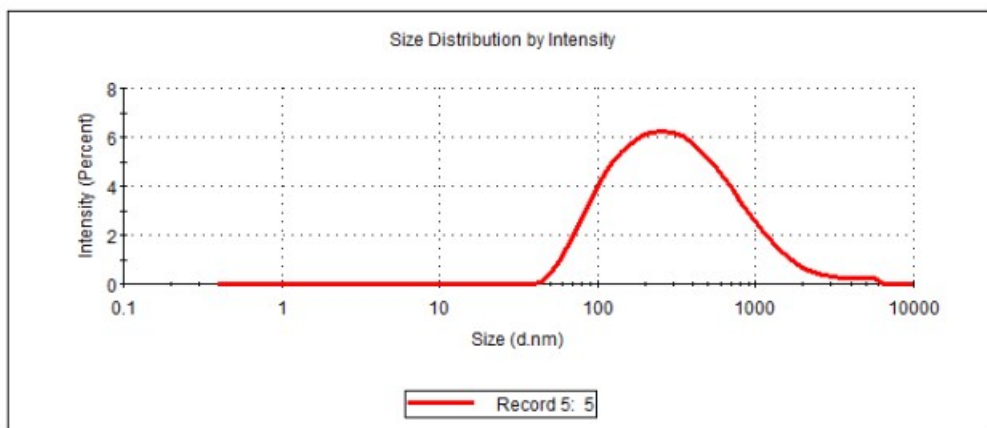


Figure S6. DLS characterizes TNPa responsive nucleolin assembly.

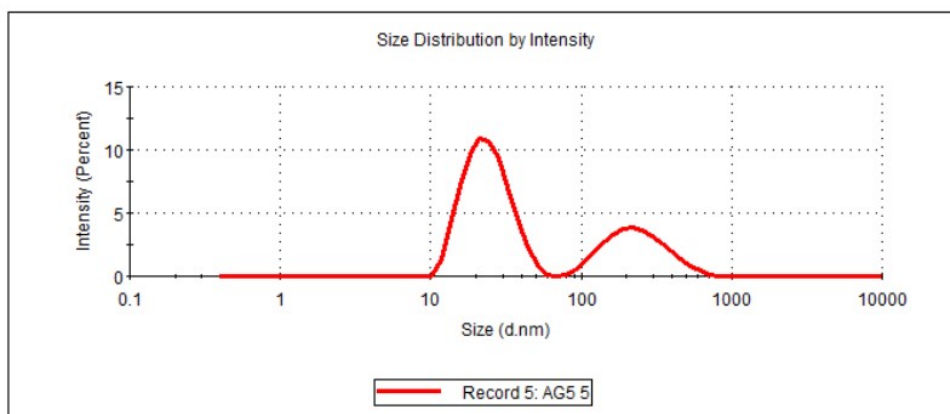


Figure S7. DLS characterization of TNPa assemblies in response to APE1 disassembly.

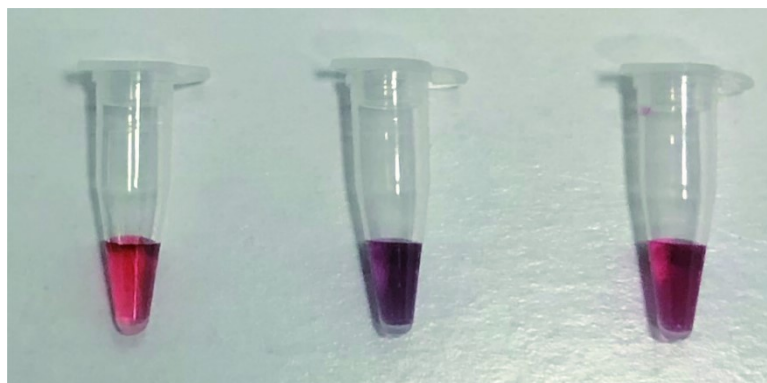


Figure S8. Colorimetric verification of TNPa assembly and disassembly processes, a: TNPa, b: TNPa + nucleolin, c: TNPa + nucleolin + APE1.

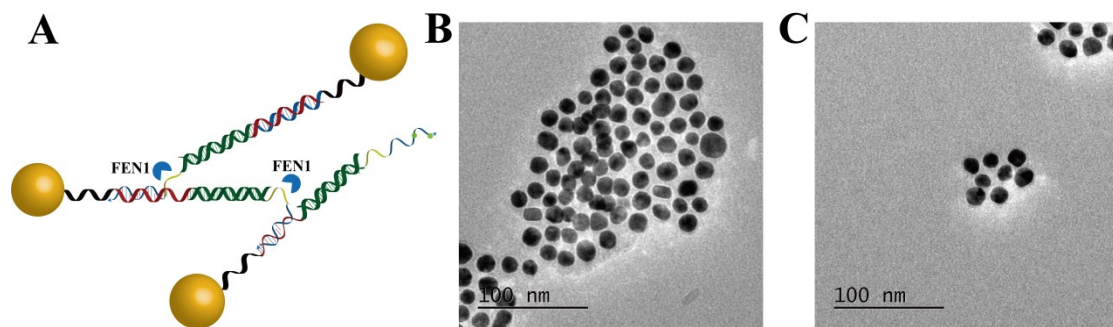


Figure S9. (A) Schematic of cleavage site of FEN1. (B) TEM of TNPa responsive TK1 mRNA assembly. (C) TEM of TNPa responsive TK1 mRNA is assembled and then disassembled in response to FEN1.

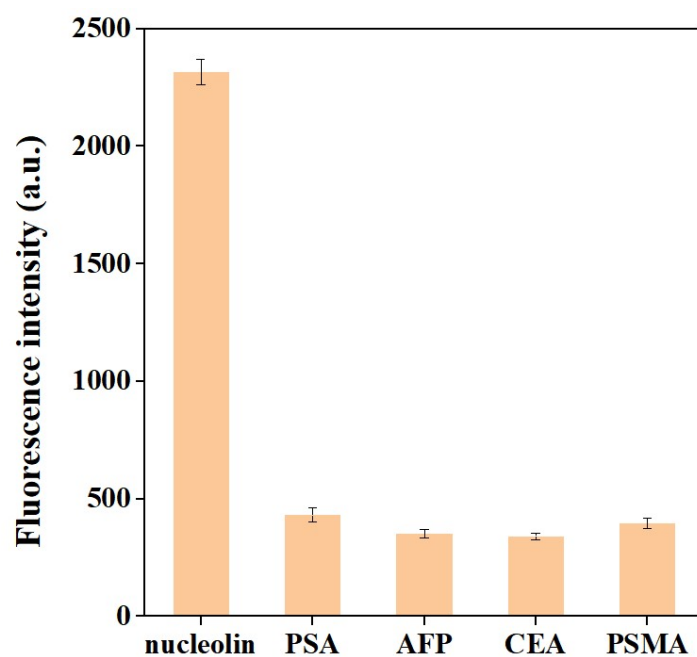


Figure S10. Selectivity of TNPa for nucleolin, a: control, b: PSA (prostate specific antigen), c: AFP (alpha-fetoprotein), d: CEA (carcinoembryonic antigen), e: PSMA (prostate-specific membrane antigen).

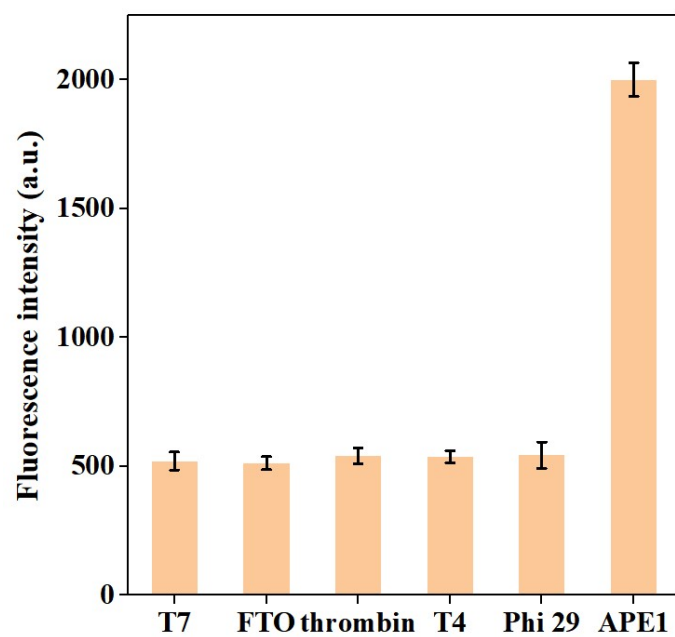


Figure S11. Selectivity of TNPa disassembly for APE1, T7: T7 endonuclease I, FTO: fat mass and obesity-associated protein, thrombin, T4: T4 DNA ligase, Phi 29: phi29 DNA polymerase.

sample	added (nM)	mean measured (nM)	mean recovery (%)	relative standard deviation (%)
1	0	not detected		
2	1	0.96 ± 0.02	95.9	1.58
3	10	10 ± 0.56	102.9	3.30
4	100	100 ± 3.66	100.3	2.12

Recovery = $(C_{\text{measured}}/C_{\text{added}}) \times 100\%$.

Table S2. Detection results of nucleolin spiked in human serum samples.

sample	added (U×10 ⁻³)	mean measured (U×10 ⁻³)	mean recovery (%)	relative standard deviation (%)
1	0	not detected		
2	1	0.96 ± 0.05	96.5	1.76
3	10	10 ± 1.56	101.1	3.30
4	100	100 ± 3.69	100.3	3.25

Recovery = (C_{measured}/C_{added}) × 100%.

Table S3. Detection results of APE1 spiked in human serum samples.

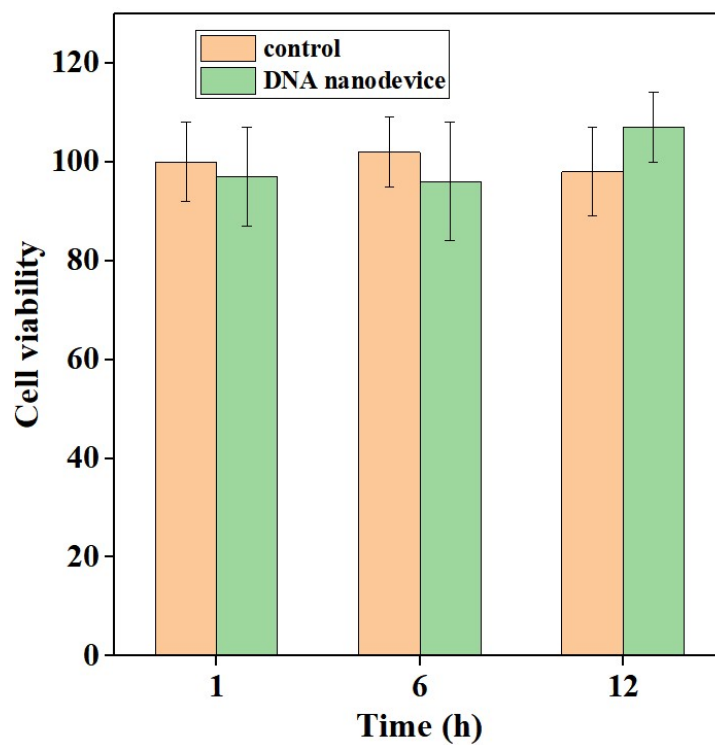


Figure S12. Viability of cells incubated with different times of 3 nM DNA nanodevice.

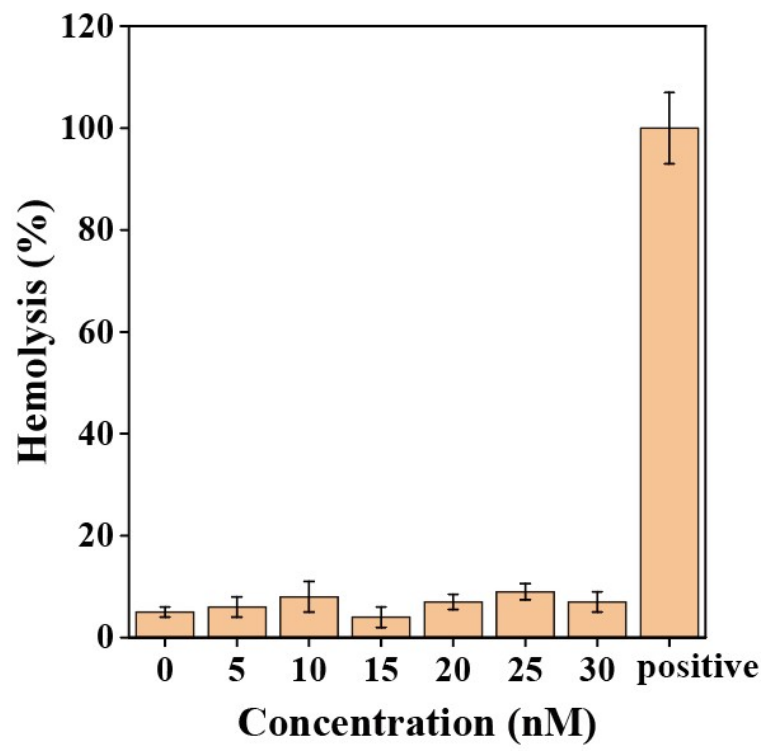


Figure S13. Hemolysis analysis the biocompatibility of TNPa.

We measured the content of nucleolin in HeLa cells using a nucleolin assay kit to be 20.96 nM, and the APE1 assay kit measured the content of APE1 in HeLa cells to be 3.11×10^{-4} U. Next, we validate the monitoring ability of TNPa for nucleolus and APE1 in solution phase at this concentration. As shown in Figure S14, 20.96 nM nucleolin can activate TNPa (line a) and achieve APE1 detection within the concentration range of 1.0×10^{-4} - 5×10^{-4} U (line b-e). It can be seen that the concentration of nucleolin in the cell can activate TNPa and achieve detection of intracellular APE1.

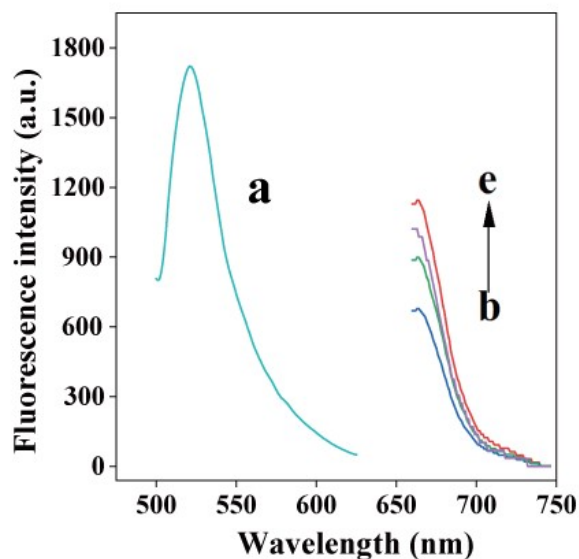


Figure S14. Fluorescence recovery curves (line a) at TNPa detection of cell nucleolin concentration, as well as detection curves of APE1 (line b-e: $1.0, 2.0, 3.0, 4.0 \times 10^{-4}$ U) at different concentrations at this concentration.

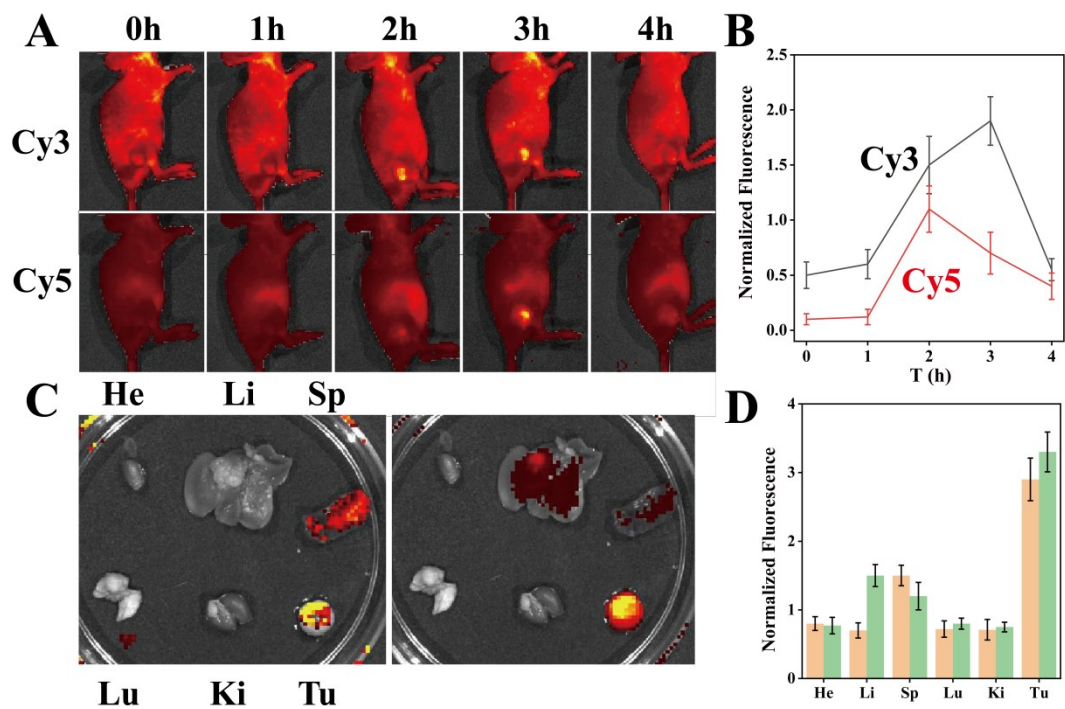


Figure S15. (A) Representative whole-body fluorescence images of tumor-bearing mice tail vein injected with TNPa. (B) Fluorescence intensity of tumor sites in Figure S15A, the green line represents the Cy3 fluorescence over time curve, the red line represents the Cy5 fluorescence over time curve. (C) Fluorescence images of ex vivo organs and tumors harvested at 4 h after TNPa injection. He, Li, Sp, Lu, Ki, and Tu stand for heart, liver, spleen, lung, kidney, and tumor, respectively. (D) Fluorescence quantification of different organs and tumors in Figure S15C.